Iranian Journal of Medical Physics

ijmp.mums.ac.ir

IJMP

The Measurement of Neutron Contamination in High Energy X-Ray Radiotherapy Using a He-3 Gas Dosimeter

Alireza Vejdani Noghreiyan[1], Mahdi Momennezhad[2], Sara Mohammadi[3], Atefeh Rostami[4], Vajiheh Vejdani Noghreiyan[4*]

1. Physics Department, Faculty of Sciences, University of Neyshabur, Neyshabur, Iran
2. Medical Physics Department, Faculty of Medicine, Imam Reza Center of Medical Education and Treatment, Mashhad, Iran
3. Medical Physics and Radiology Department, Faculty of Medicine, Gonabad University of Medical Sciences, Gonabad,Iran
4. Department of Medical Physics and Radiological Sciences, Sabzevar University of Medical Sciences, Sabzevar, Iran

ARTICLE INFO

Article type:
Original Paper

Article history:
Received: Oct. 10, 2023
Accepted: Jan 14, 2024

Keywords:
Linear Accelerator
Dosimetry
Radiation
Neutron Activation Analysis

ABSTRACT

Introduction: Neutron contamination is likely caused by the collision of high-energy photon interactions (γ, n) with heavy metals used in the construction of the accelerator. This study is essential to quantify the excess dose from neutron contamination by Elekta Precis. The main object is to assess the neutron contamination with a gas dosimeter containing He-3.

Material and Methods: In this study, neutron contamination was estimated at different points in and out of the treatment room. We used two types of dosimeters: a He-3 gas dosimeter (CRAMAL 31) as a neutron dosimeter and Farmer ionization chambers, and PC-electrometer (Sun Nuclear, USA) which is sensitive to photons measured photo-neutron doses. Both the neutron and Farmer dosimeters were applied in the presence and absence of acrylic plates at the same point. In this study, Monte Carlo (MC) code was utilized to prepare the correct proportion of neutron dose.

Results: At different points in and out of the treatment room, neutron contamination was approximately in the range of background dose (D = 0.001 µSv). The neutron dosimeter displayed 48.792 µSv, 25.456 µSv and 28.756 µSv for 6, 10 and 15 MV photon energy, respectively. He-3 gas dosimeter showed that the neutron dose net was negligible under the treatment field.

Conclusion: He-3 gas dosimeter detected more than the usual neutron dose in 6 MV photon energy than we expected. Due to the high photon flux under the radiation fields, a He-3 neutron dosimeter reported photo-neutron dose. Nevertheless, the photo-neutron dose was in the range of micro Sievert (µSv). He-3 gas dosimeter was not suitable for neutron dosimetry in places with high photon fluence because of the low energy peak in the detection of neutrons.

► *Please cite this article as:*
Vejdani Noghreiyan A, Momennezhad M, Mohammadi S, Rostami A, Vejdani Noghreiyan V. The Measurement of Neutron Contamination in High Energy X-Ray Radiotherapy Using a He-3 Gas Dosimeter. Iran J Med Phys 2024; 21: 329-335. 10.22038/ijmp.2024.75447.2332.

Introduction

In radiotherapy, the most common type of treatment is using photons and electrons in external beam radiotherapy (EBRT). By using this type of treatment, electrons are accelerated by linear accelerators (LINACs), and then a collision with a metal target produces high energy X-ray photons [1]. The range of photon energy used in medical accelerators for cancer treatment is usually between 4 and 20 MV. The interactions between high energy photons (>8 MV) and high Z materials used in LINAC structures can cause neutron contamination which should be considered as the most crucial issue [2]. Generated neutrons can cause an additional dose received to a patient and staff. Neutron contamination produced by LINAC structures are from: the walls of the vacuum chamber, the walls of the waveguide, the flattening filter, and the asymmetric jaws [3]. In addition the walls of the treatment room can be sources of neutron contamination. NCRP reports 79 and 102 recognized the importance of neutron contamination in medical LINACs [4,5].

There is much evidence showing that a reasonable relation exists between neutron contamination and the accelerator type (energy generation, target ingredients), the facility's topology like maze shape, beam orientation, composition and thickness of the door and walls, position of the console control panel and the therapy technique like conventional, conformal or intensity modulated and somethings related to treatment planning (monitor units, field size, collimation, etc.) [6-9]. Another method that has the potential to produce neutron contamination is the nuclear reaction between the patient body and photon beam, although it is negligible in comparison with the neutron contamination by the head of LINAC [10,11]. Even when the organs at risk are outside of the

*Corresponding Author: Tel: +98-9105000085; Fax: +98-5138002320; Email: vajihehvn@yahoo.com

treatment field, neutrons may still be the main cause of damage. [12].

As reported by Wen-Shan Liu [13], the thermal neutron fluence was measured by the technology of activating indium foil. In this type of dosimeter, the presence of a neutron activates indium then gamma rays are emitted. In this way, the number of gamma emitted is equally considered as the number of thermal neutrons. Another dosimeter used in radiotherapy is TLD (Thermo Luminescent Dosimeter) [14-16], especially in neutron contamination [17-19]. All these studies mentioned the fact that neutron contamination causes extra dose production so it should be considered.

Neutron contamination plays an important role in biological effects. The biological effect of neutrons is substantially greater than that of photons because of their high radiation weighting factor (WR) provided in International Commission on Radiological Protection (ICRP) report No. 60 [20], so low doses of neutrons can lead to significant biological effects. One of the main reasons for developing a second cancer in patients is absorption of undesired neutrons produced by medical LINACs [21,22].

While there are various studies on neutron contamination from different accelerators, to the best of our knowledge, there have been no reports of neutron contamination in less than 8 MV photon energy. So in this current study, 6, 10 and 15 MV of photon beam energy produced by the Elekta (Precise) linear accelerator was investigated. Additionally, we analyzed the neutron contamination counted with a gas dosimeter (Helium-3), which is a reliable dosimeter in nuclear reactors with high neutron fluence. This study shows how good the helium-3 dosimeter is in the treatment area with high gamma fluence.

Materials and Methods

In this study, Elekta (Elekta Precise®, Stockholm) linear accelerator with photon beam energies of 6, 10 and 15 MV was investigated at the radiotherapy department of Imam Reza Hospital in Mashhad. Determining the neutron contamination in the treatment fields, different areas inside and outside the treatment room and the Linac control room was conducted.

Radiation detectors require ionizing radiation that interact with atomic electrons and either ionize or excite atoms. Neutrons do not interact with electrons. Therefore only nuclei must use nuclear reaction in a detector to detect neutrons. CRAMAL 31 is a kind of neutron dosimeter containing He-3, which has a large cross-section of neutron interactions and is most commonly used in measuring neutron pollution in the environment (Figure 1). A gas dosimeter (CRAMAL 31 code 18396; Canberra, Meriden, CT) which was used to measure the neutron dose, is a portable digital instrument. It can be used for radiation protection in facilities involving risks of irradiation from neutrons and, in particular, nuclear power plants, other reactors, accelerators, etc. This dosimeter is filled by Helium-3 gas, which has a high cross-section with neutrons.

The epithermal neutrons are detected in accordance with the following nuclear reaction [30]:

$$^{3}_{2}He + \, ^{1}_{0}n \rightarrow \, ^{1}_{1}H + \, ^{3}_{1}H + 764 \, keV$$

A Helium-3 proportional counter placed beneath Cadmium at the center of a 20 cm diameter polyethylene sphere acted as a moderator (Figure 2).

This arrangement shows the low sensitivity in high neutron energies. It has the most sensitivity in 3 MeV neutron energy and it can detect a minimum energy of approximately 0.5 keV. Calibration was performed at the Secondary Standard Dosimetry Laboratory (SSDL) (Karaj, Iran).

By reviewing several studies in relation to the photon response of this dosimeter, no reports have been observed. Therefore, in this study to enhance the measurement accuracy, the photon sensitivity of this dosimeter was also investigated.

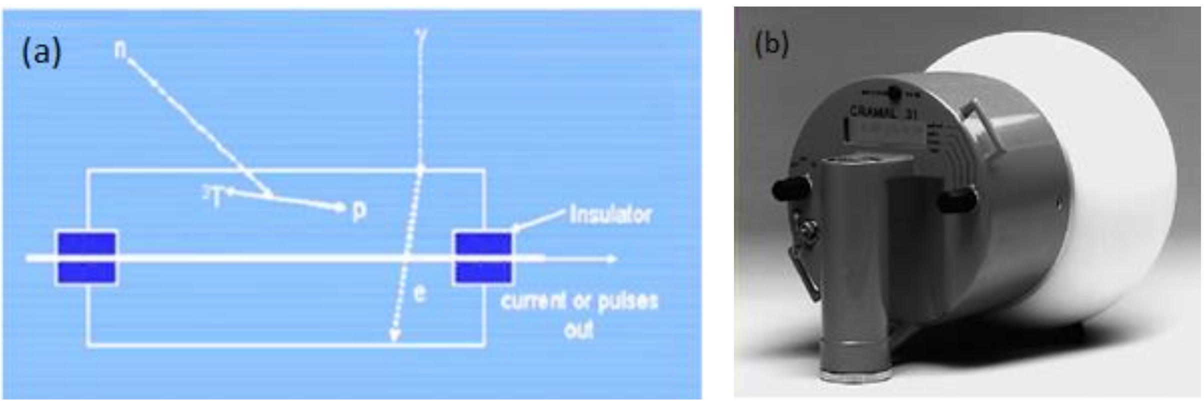

Figure 1 (a): the cuurent or pulses out by the intraction of ^{3}He and n (b): ^{3}He filled I

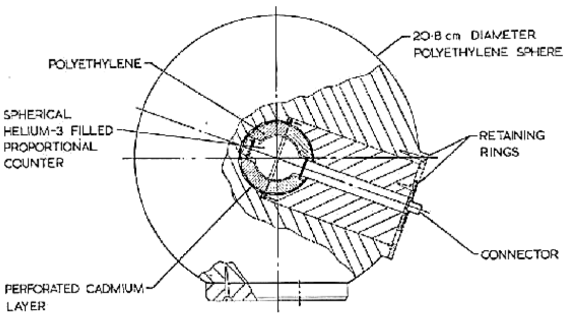

Figure 2. Spherical neutron dosimeter based on a ^{3}He neutron detector

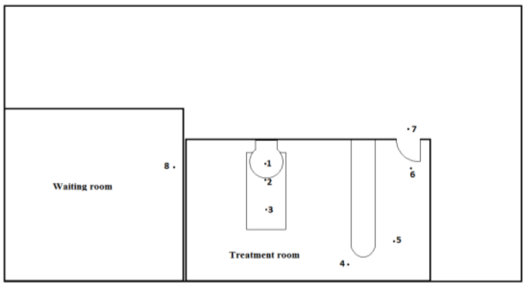

Figure 3. The structure of the treatment room

At the first step of our measurements, the neutron dosimeter was placed at eight different points (in and out of the treatment room) (Figure 3). The point 1 shows the Isocenter, the point 2 and the point 3 are 12 centimeters and 110 centimeters far from the Isocenter. The point 4 and the point 5 are the maze. The point 6 shows the neutron doses in the treatment room while the point 7 shows the neutron doses out the treatment room considered as Linac control room. The point 8 was measured as a point in waiting room because of the presence of lead in the wall. The distance of neutron dosimeter and the floor was 110 cm to measure the scatter dose produced by the floor. It was irradiated by 100 cGy with three photon energies of 6, 10 and 15 MV. In order to obtain a correction factor of neutron count, Farmer dosimeter (PTW TM30012 Farmer chamber) and PC-electrometer (Sun Nuclear, USA) and acrylic plates ($C_5H_8O_2$ with the density of 1.18 g/cm3) were used. Farmer dosimeter is sensitive only to photons and acrylic plates have high cross sections with neutrons which leads to neutron capture.

In the second step of our measurements, Farmer dosimeter was irradiated by photons with and without the acrylic plates in a constant dose (100 cGy) (Figure 4). Under the same condition, neutron dosimeter was also irradiated by photons as well. The neutron dosimeter was irradiated with four different doses (monitor units) to show linearity behavior (Figure 5).

Measured dose by Farmer and neutron dosimeters showed photon and photon-neutron doses, respectively. Using the 5 acrylic plates that each has a thickness of 1 cm can obviously reduce photon and neutron-photon doses. Simultaneously, Monte Carlo (MC) code was used to illustrate how acrylic plates can reduce the gamma fluence in both gamma and neutron dosimeters. For this purpose, first the MCNPX-2.6 code was used to generate the phase space (PS) distributions by simulating the head of Elekta SL-25 linac collimation system based on manufacturer's detailed information. Generated PS files were used to define source in all of the next simulations. The F1 tally was used to calculate the number of gamma rays reached to a defined square as a cell in the presence of 5 cm acrylic plates. The distance between cell and plates was considered about 50 cm. Two MCNPX programs were run in neutron and photon modes. PHYS:P was used in order to take into account the photo neutron production by setting ispn=-1 and the upper energy limit for detailed photon physics treatment was set to 20 MeV. To take into account delayed gamma rays caused by neutron activation in PHYS:P card dgb was set to -101. PHYS:P 20 1 0 -1 1 -101. For PHYS:N all the parameters were set to default except for emax (upper limit for neutron energy which was set to 10 MeV. PHYS:N 10 0 0 -1 -1 0 0. The relative errors of our Monte Carlo results were less than 1%.


Figure 4. Farmer dosimeter with and without acrylic plates

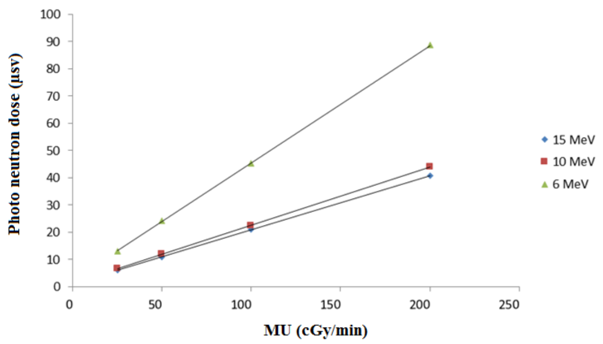

Figure 5. Linearity behavior of the neutron dosimeter

Results

In this research, photons 6, 10, and 15 MV were used. The results Tables 1, 2 show that the neutron fluence increases with photon energy and decreased by moving away from the isocenter. These tables illustrate that the photo-neutron dose increases in the treatment room by limiting the beam by collimators. We observed an unexpected result. According to Table 3, the neutron dosimeter response was observed at 6 MV.

Table 1. Photoneutron dose in different points of treatment room inside and outside Photon energy = 15 MV

Dosimeter position	Neutron dose (µsv)	Field size (cm^2)	Gantry angle (degree)
Point 1	28.756	20*20	0
Point 1	21.634	40*40	0
Point 2	31.258	20*20	0
Point 2	29.712	40*40	0
Point 3	28.731	20*20	0
Point 3	8.403	20*20	270
Point 3	11.087	20*20	90
Point 4	9.426	20*20	0
Point 4	16.895	20*20	270
Point 5	0.001	20*20	0
Point 5	0.358	20*20	270
Point 6	0.001	20*20	0
Point 6	0.001	20*20	270
Point 6	0.001	40*40	270
Point 7	0.001	40*40	270
Point 7	0.001	20*20	270
Point 8	0.001	20*20	90
Point 8	0.001	40*40	90

Point 1: Isocenter, point 2: 12 centimeters from Isocenter, point 3: 110 centimeters from Isocenter, point 4: maze

Table 2. photoneutron dose in different points of treatment room inside and outside. Photon energy = 10 MV

Dosimeter position	Neutron dose (µsv)	Field size (cm^2)	Gantry angle (degree)
Point 1	25.456	20*20	0
Point 1	23.963	40*40	0
Point 2	31.258	20*20	0
Point 2	23.557	40*40	0
Point 3	23.123	20*20	0
Point 3	4.563	20*20	270
Point 3	9.632	20*20	90
Point 4	6.489	20*20	0
Point 4	7.884	20*20	270
Point 5	0.001	20*20	0
Point 5	0.001	20*20	270
Point 6	0.001	20*20	0
Point 6	0.001	20*20	270
Point 6	0.001	40*40	270
Point 7	0.001	40*40	270
Point 7	0.001	20*20	270
Point 8	0.001	20*20	90
Point 8	0.001	40*40	90

Table 3. Photoneutron dose in different points of treatment room inside and outside. photon energy = 6 MV

Dosimeter position	Neutron dose (µsv)	Field size (cm^2)	Gantry angle (degree)
Point 1	48.792	20*20	0
Point 2	40.531	20*20	0
Point 3	31.823	20*20	0

The results in Table 4 and Table 5 show the reduction in the photo-neutron and photon doses in the presence and absence of acrylic plates inside the treatment field.

By the simply simulation, the results (Table 6) illustrate that the gamma fluence was roughly constant in the presence and absence of acrylic plates at all three energies. However, the neutron fluence decreased by an order of %55 at the photon energy 15 MV.

Table 4. Measured dose by neutron dosimetry in gantry angel zero and field size 20*20

	Photo-Neutron dose (µsv) without acrylic		Photo-Neutron dose (µsv) with acrylic	
	100 Mu*	200 Mu	100 Mu	200 Mu
15 MV	21.001	40.819	20.863	39.916
	20.726	41.331	20.128	40.56
10 MV	22.48	44.102	22.535	43.956
	22.681	43.786	22.965	43.614
6 MV	45.302	88.675	46.265	90.543
	47.712	89.816	46.895	90.963

*Monitor unite

Table 5. Measured dose by Farmer in gantry angel zero and field size 20*20

	without acrylic		with acrylic	
	Count (nC*)	Photon dose (Gy)	Count (nC)	Photon dose (Gy)
15 MV	-18.38	0.881	-15.92	0.764
	-18.38	0.881	-15.93	0.764
10 MV	-18.25	0.876	-15.41	0.739
	-18.26	0.876	-15.41	0.739
6 MV	-17.49	0.838	-14.09	0.676
	-17.48	0.838	-14.09	0.675

* nanocoulomb

Table 6. Simulation of gamma fluence in gantry angel zero and field size 20*20

without acrylic		with acrylic
	Photon dose (Gy)	Photon dose (Gy)
15 MV	0.125	0.124
10 MV	0.125	0.122
6 MV	0.125	0.121

Discussion

In some studies [23,24], it is noted that medical accelerators that produces photons with energies higher than 8 MV impose an unwanted dose due to neutron contamination. The problem getting worse when high-density materials as metal are used in the walls for shielding photons but interact with photons and become a sources of photo-neutron (point 8 in Figure 3) The neutron dose at eight different points in the treatment room (shown in Table 1) is in good agreement with the other reports of LINACs photo-neutron contamination [25-28].

According to Table 3, the neutron dosimeter response was observed at 6 MV. According to data, the threshold energies to produce neutron contamination related to tungsten and lead are 6.2 and 6.7 MV respectively, so the presence of these elements in the accelerators structure even at lower energy than 10 MV can also produce neutron contamination [29].

As we showed in Table 4 and Table 5, the neutron dose did not change in the presence and absence of acrylic plates but these conditions changed the photon dose to Farmer between 13% and 19%.

The simulation results indicate that the presence of the acrylic plates did not reduce the gamma fluence, but reduced gamma energy. According to Table 5, photons attenuation in presence of acrylic plates was 13% and 19% for photon energies 15 and 6 MV, respectively. So by reducing the energy, the effect of the presence and absence of acrylic plates is much greater in photon dose.

If the plates cannot change the fluence, the neutron dosimeter, which is highly dependent on the gamma fluence, should not be changed. So the data in Table 4 confirm this fact.

According to Table 4, the photo-neutron dose measured by the neutron dosimeter was roughly constant with and without acrylic plates. On the other hand, the simulation results showed 55% decrease in the neutron dose under the same conditions. So, we can conclude that the portion of the neutron dose in photo-neutron dose (the numbers which neutron dosimeter showed) was negligible. So that with the reduction of 55% in the neutron dose, we observed constant measurements.

When the neutron dosimeter is placed in a high gamma fluence (usually at the isocenter), the electrons are detached from the aluminum wall. Each electron can cause a few ionizations along the path and generates a small voltage peak in the dosimeter so the integration of some peaks can be considered as a neutron entry and a neutron count. So in the condition of a high fluence of gamma or isocenter, the neutron peak is generated by overlapping small peaks of wall electron ionization. The voltage peak to consider neutron dose is 764 keV for a He-3 detector so that it is lower than neutron voltage peak in BF3 dosimeter that is approximately 2 MeV [30].

The data illustrate that neutron dose at energy photon 6 MV is approximately 2 times greater than that at energy photon 15 MV. This is confirmed by the above reason. At both photon energies of 6 and 15 MV we had a constant dose rate (400 Mu/min) so to obtain the specific dose to surface (Source to surface distance SSD=100 cm) the photon fluence at lower energy should be greater. According to this fact, by increasing the photon fluence, the amount of wall electron ionization increased.

Conclusion

CRAMAL 31 has high sensitivity of the neutrons detection with a maximum energy of 2 MV. So, it is proper in a condition with high neutron fluence and limited energy.

According to the results, He-3 has a higher cross-section for thermal neutrons than BF3 but due to the high fluence of the gamma in the isocenter, the use of the He-3 dosimeter is not accurate. The neutron dosimeter (He-3) is suitable under a maximum dose rate 100 rad/ hour, so in the other points of the treatment room, where the gamma fluence is reduced to 2 rad/ hour, the neutron dosimeter shows the actual dose.

Although the doses measured inside the treatment field were a combination of photon and neutron doses, they are well confirmed to the photo-neutron dose reported in published papers.

This paper has demonstrated that although the He-3 dosimeter is not suitable for a condition with high gamma fluence to measure the absolute dose of neutrons, it can be used for other places in the treatment room.

Acknowledgment

The authors would like to extend their highest gratitude to the radiation oncology department of Imam Reza Hospital for allowing us to use their systems and their sincere cooperation

References

1. Evans E, Staffurth J. Principles of cancer treatment by radiotherapy. Surgery (Oxford). 2018;36(3):111-6.
2. Banaee N, Goodarzi K, Nedaie HA. Neutron contamination in radiotherapy processes: a review study. Journal of Radiation Research. 2021; 62(6):947-54.
3. Farrag EA, Wadi-Ramahi S, Hamad MK. Photo-neutron production of medical linear accelerator Elekta, precise model: A study with the Geant4 MC toolkit. Annals of Nuclear Energy. 2023 Dec 15;194:110136.
4. NCoRP N. Neutron Contamination from Medical Linear Accelerators. NCRP Report 79. 1984.
5. NCoRP N. Medical X-ray, Electron and Gamma-Ray Protection for Energies up to 50 MeV. NCRP Report 102. 1989.
6. Donadille L, Trompier F, Robbes I, Derreumaux S, Mantione J, Asselineau B, et al. Radiation protection of workers associated with secondary neutrons produced by medical linear accelerators. Radiation Measurements. 2008;43(2-6):939-43.
7. Rajesh K, Raman RG, Musthafa M, Midhun C, Joseph N. A passive method for absolute dose evaluation of photoneutrons in radiotherapy. International Journal of Radiation Research. 2020;18(1):173-8.
8. Noghreiyan VV, Naseri S, Momennezhad M. Utilization of Electronic Portal Imaging Device (EPID) For Setup Verification and Determination of Setup Margin in Head and Neck Radiation Therapy. Iran J Med Phys. 2020 May 1;17(3):198.
9. Banaee N, Goodarzi K, Hosseinzadeh E. Comparison of neutron contamination in small photon fields of secondary collimator jaws and circular cones. Journal of Radiotherapy in Practice. 2023 Jan;22:e107.
10. Al-Ghamdi H, Al-Jarallah M, Maalej N. Photoneutron intensity variation with field size around radiotherapy linear accelerator 18-MeV X-ray beam. Radiation measurements. 2008;43:S495-S9.
11. Saeed MK, Moustafa O, Yasin O, Tuniz C, Habbani F. Doses to patients from photoneutrons emitted in a medical linear accelerator. Radiation protection dosimetry. 2009;133(3):130-5.
12. Horst F, Fehrenbacher G, Zink K. On the neutron radiation field and air activation around a medical electron linac. Radiation protection dosimetry. 2017;174(2):147-58.
13. Liu W-S, Changlai S-P, Pan L-K, Tseng H-C, Chen C-Y. Thermal neutron fluence in a treatment room with a Varian linear accelerator at a medical university hospital. Radiation Physics and Chemistry. 2011;80(9):917-22.
14. Bahreyni Toossi MT, Gholamhosseinian H, Vejdani Noghreiyan A. Assessment of the effects of radiation type and energy on the calibration of TLD-100. Iranian Journal of Medical Physics. 2018;15(3):140-5.
15. Ebrahimi-Khankook A, Vejdani-Noghreiyan A, Ziyaei-Laeen S. Investigation of the effect of using radiation protective glasses on the photon fluence-to-dose conversion coefficients of eye substructures. Journal of Radiological Protection. 2021;41(4):1093.
16. Soleymanifard S, Toossi MTB, Khosroabadi M, Shahidsales S, Tabrizi FV. Assessment of skin dose modification caused by application of immobilizing cast in head and neck radiotherapy. Australasian physical & engineering sciences in medicine. 2014;37(3):535-40.
17. Khajetash B, Toossi MTB, Ghorbani M, Jahangiri M, Akbari F. Measurement of fast neutron contamination caused by the presence of wedge and block using CR-39 detector. Journal of Cancer Research and Therapeutics. 2019;15(8):S103-S9.
18. Mohammadi S, Behmadi M, Mohammadi A, Toossi MTB. Thermal and fast neutron dose equivalent distribution measurement of 15-mv linear accelerator using a CR-39 nuclear track detectors. Radiation protection dosimetry. 2020;188(4):503-7.
19. Banaee N, Goodarzi K, Nedaie HA. Neutron contamination in radiotherapy processes: a review study. Journal of Radiation Research. 2021;62(6):947-54.
20. Thorne M. ICRP publication 60: 1990 recommendations of the international commission on radiological protection: Annals of the ICRP, 21 (1–3), 1991. Pergamon; 1992.
21. Toossi MB, Khajetash B, Ghorbani M. Assessment of Neutron Contamination Originating from the Presence of Wedge and Block in Photon Beam Radiotherapy. Journal of Biomedical Physics and Engineering. 2018;8(1):3.
22. Schneider U, Fiechtner A, Besserer J, Lomax A. Neutron dose from prostheses material during radiotherapy with protons and photons. Physics in Medicine & Biology. 2004;49(9):N119.
23. Zanini A, Durisi E, Fasolo F, Ongaro C, Visca L, Nastasi U, et al. Monte Carlo simulation of the photoneutron field in linac radiotherapy treatments with different collimation systems. Physics in Medicine & Biology. 2004;49(4):571.
24. Martinez-Ovalle S, Barquero R, Gomez-Ros J, Lallena A. Neutron dose equivalent and neutron spectra in tissue for clinical linacs operating at 15, 18 and 20 MV. Radiation protection dosimetry. 2011;147(4):498-511.
25. Choi CH, Park S-Y, Park JM, Chun M, Kim J-i. Monte Carlo simulation of neutron dose equivalent by photoneutron production inside the primary barriers of a radiotherapy vault. Physica Medica. 2018;48:1-5.
26. Dawn S, Pal R, Bakshi A, Kinhikar R, Joshi K, Jamema S, et al. Evaluation of in-field neutron production for medical LINACs with and without flattening filter for various beam parameters-Experiment and Monte Carlo simulation. Radiation Measurements. 2018;118:98-107.

27. Nourmohammadi B, Mesbahi A. A Review on the Radiation Therapy Technologist Received Dose from Induced Activation in High-Energy Medical Linear Accelerators. Radiation protection dosimetry. 2018; 179(4):333-48.
28. Kim J-H, Seo J-M, Kim G-J. Analysis on the photoneutron according to the varying factors and treatment planning in LINAC. Optik-International Journal for Light and Electron Optics. 2018;156:424-32.
29. Chin MP. Neutron contamination in a radiotherapy maze. Master's thesis, University of Surrey. 1999.
30. Knoll GF. Radiation detection and measurement: John Wiley & Sons; 2010.